Path-Tracking Control Strategy for Enhanced Comfort in All-Wheel-Steering Autonomous Vehicles

Lin, Chenhui; Papaioannou, Georgios; Siampis, Efstathios; Velenis, Efstathios

DOI
10.1007/978-3-031-66968-2_32

Publication date
2024

Document Version
Final published version

Published in
Advances in Dynamics of Vehicles on Roads and Tracks III

Path-Tracking Control Strategy for Enhanced Comfort in All-Wheel-Steering Autonomous Vehicles

Chenhui Lin[1(✉)], Georgios Papaioannou[2], Efstathios Siampis[1], and Efstathios Velenis[1]

[1] Advanced Vehicle Engineering Centre, Cranfield University, Cranfield MK43 0AL, UK
chenhui.lin@cranfield.ac.uk

[2] Cognitive Robotics Department, Delft University of Technology, 2600 AA Delft, Netherlands

Abstract. In this paper, a path-tracking controller is developed for an autonomous vehicle with All-Wheel-Steering (AWS) capability. Based on nonlinear model predictive control, the proposed controller is formulated in a way that allows the manipulation of vehicle's attitude during path-tracking. With high-fidelity vehicle dynamics simulation, the controller is examined at various velocities up to the limit handling condition. Comparison is carried out in the aspects of path-tracking, ride comfort and motion sickness, between the implementation with a constant yaw angle reference (referred to as crab steering) and the nominal steering behaviour for negotiating the same path. The ride comfort metric suggested by ISO-2631 is used to capture the benefits of the crab steering approach against the nominal case, and the simulation results reveal that crab steering is able to enhance the ride comfort for AWS vehicles in double lane-change and slalom manoeuvres.

Keywords: Autonomous vehicle · Path-tracking · All-wheel steering · Ride comfort

1 Introduction

The past decade has witnessed a significant stride with regards to the development of Autonomous Vehicle (AV) technologies. In the topic of path-tracking, different control methods have been applied to address the path-tracking problem [1]. Among these approaches, Nonlinear Model Predictive Control (NMPC) has been recognized as an outstanding technique. Rokonuzzaman et al. evaluated and compared seven different control techniques for path-tracking of AVs [2]. The simulation results demonstrated that optimization-based controllers such as LQR and NMPC achieved better path-tracking performance than the other controllers, while NMPC provided better robustness due to the utilization of nonlinear models. Furthermore, model predictive control has also shown its advantage in dealing with constraints such as system limitations and road boundaries [3].

W. Huang and M. Ahmadian (Eds.): IAVSD 2023, LNME, pp. 325–335, 2024.
https://doi.org/10.1007/978-3-031-66968-2_32

With the development of active chassis control techniques such as Torque-Vectoring (TV) and All-Wheel Steering (AWS), advanced driver assist functionalities have been enabled to improve safety and driving experience [4,5]. With regards to AVs, the available multi-actuation can be deployed especially at the path-tracking level to achieve enhanced performance. Research has shown that the application of multi-actuation can exploit the vehicle's dynamical capability under demanding scenarios [6,7], and can therefore improve the handling performance of AVs. However, less work has been done on evaluating how the riding experience can also be affected with multi-actuation.

AVs have been acknowledged as the next generation of road transportation, and they are expected to improve traffic efficiency as well as road safety. In the upcoming era of autonomous driving, human drivers may no longer be necessary, which means that the requirements for subjective driving feel can be neglected. On the other hand, the absence of human drivers also leads to a potential risk of neglecting occupants' motion comfort [8]. One of the advantages of AVs is to allow passengers to carry out a wide variety of non-driving tasks, which on the other hand may draw their attention from anticipating vehicle behaviours, leading to increasing possibility of motion sickness. Hence, ride comfort and motion sickness should also be included in the evaluation of AV performance.

In terms of path-tracking, most of the work that has been carried out lays the emphasis on improving stability and minimising tracking error, while path-tracking can also be optimized against the metrics focusing on riding experience of passengers. In [9], an extended MPC strategy was presented for path-tracking of AVs, and was validated in hardware-in-the-loop simulation. The controller was constructed to achieve smoother path-tracking and better ride comfort than conventional MPC strategies, while it was based on a linearized bicycle model with front-wheel steering, so the performance could not be guaranteed close to the limit handling conditions. In [10], a path-tracking controller was developed for autonomous vehicles with four-wheel drive and steering, and analysis was given that four-wheel steering helped to improve the ride comfort. However, such conclusion was drawn according to the evaluation of ride comfort based on side slip angle, which may not reflect the actual situation.

In this paper, we present a nonlinear predictive path-tracking controller, taking advantage of the available TV and AWS capabilities of a modern electric AV platform. The controller is designed to address a broad range of operating conditions, including the limit handling condition of the vehicle. Using high-fidelity simulation, we illustrate the flexibility of the proposed control formulation in enabling different strategies for negotiating typical high speed transient manoeuvres, particularly with regards to control of vehicle's posture. Apart from nominal steering behaviour, the vehicle's attitude can be manipulated by providing a constant yaw angle reference to the controller, which is referred to as crab steering. The controller with both nominal steering and crab steering strategies are examined and compared, and simulation results reveal the benefits of the crab steering strategy in improving ride comfort in double lane-change as well as slalom manoeuvres.

2 Vehicle Dynamics Modelling

The specific vehicle for control design in this work has one electric motor driving the front wheels through an open differential, while the rear wheels are driven independently by the other two motors, so that TV can be realized on the rear axle. In addition, the vehicle is equipped with steer-by-wire systems on both front and rear axles, which enables the AWS capability.

A nonlinear double-track vehicle model is used for the development of the proposed path-tracking controller. Figure 1 shows a schematic diagram of the vehicle model, where V_x and V_y stand for longitudinal and lateral velocity, and r refers to the yaw rate of the vehicle at its Centre Of Gravity (COG); l_F and l_R are the distances from the front and rear axle to COG; w_L and w_R are length of the left and right segments of the track width separated by COG. The steering angles on the front and rear wheels are denoted by δ_F and δ_R respectively, and f_{ijk} $(i = F, R,\ j = L, R,\ k = x, y)$ stands for the tyre force at the specific tyre and direction. Pitch, roll and heave motion of the vehicle are neglected, assuming that the vehicle travels on a horizontal plane.

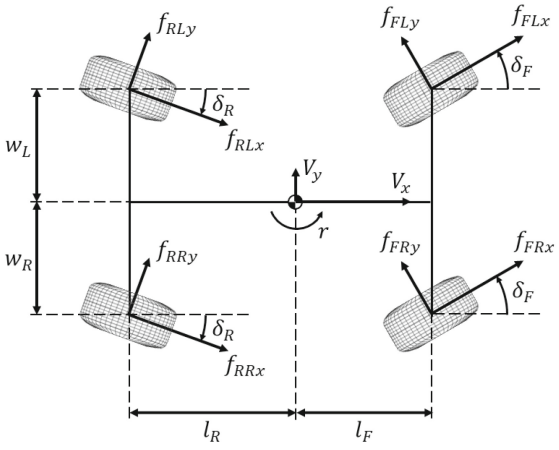

Fig. 1. Schematic diagram of the vehicle model.

To guarantee the control performance at the limits of handling, it is also necessary to apply an appropriate tyre model which takes into account the nonlinear characteristics of tyre force. With the assumption that the tyre's adhesion limit is not exceeded in the longitudinal direction, which can be realized with constraints on the driving torque inputs, the longitudinal tyre force is proportional to the driving torque applied on the wheels. A simplified Pacejka's Magic Formula tyre model is used for the modelling of lateral tyre force. Longitudinal and lateral load transfer is taken into account for calculating the dynamical vertical tyre load. The Equations Of Motion (EOM) as well as more information of the vehicle platform can be found in [11].

3 NMPC Path-Tracking Controller

For the purpose of path-tracking at a target velocity, the discrete-time NMPC optimization problem is formulated as:

$$\begin{aligned} \min_{x,u} \sum_{k=0}^{N-1} & (x_{k+1} - x_{ref,k+1})^T Q (x_{k+1} - x_{ref,k+1}) \\ & + (u_k - u_{ref,k})^T R (u_k - u_{ref,k}), \\ st. \quad & x_0 = x_{initial} \\ & x_{k+1} = f_d(x_k, u_k), k = 0, 1, \cdots, N-1 \\ & x_{min} \leq x_k \leq x_{max}, k = 0, 1, \cdots, N-1 \\ & u_{min} \leq u_k \leq u_{max}, k = 0, 1, \cdots, N-1 \end{aligned} \tag{1}$$

where x refers to the state vector $[V_x, V_y, r, X, Y, \Psi]^T$ and u stands for the control input vector $[\delta_F, \delta_R, T_F, T_{RL}, T_{RR}]^T$, in which X, Y and Ψ denote the vehicle's position and orientation expressed in Cartesian coordinates, while T_n $(n = F, RL, RR)$ refers to the torque commands for the three motors. x_{ref} and u_{ref} are the references for x and u respectively. N is the number of steps in the prediction horizon, and Q, R are the weighting matrices for x and u respectively. f_d represents the discrete-time system of the model, which is obtained by applying explicit Runge-Kutta 4th order approach to discretize the continuous-time system. Box constraints are used on the control inputs in this work, while they can easily be extended to include time-varying constraints if required.

A linear bicycle model is used for the reference generation of the steering inputs. Assuming that the vehicle is in steady state, the EOM are given in the state space form in Eq. 2, where m and I_z refers to vehicle's mass and its moment of inertia about the vertical axis through COG, while C_F and C_R are the cornering stiffness of the front and rear tyres respectively. By giving references to the steering inputs, it helps to reduce the computational time of the NMPC optimization problem, while low weighting factors are applied to avoid their dominance in the cost function.

$$\begin{aligned} \begin{bmatrix} \delta_{Fref,k} \\ \delta_{Rref,k} \end{bmatrix} = & - \begin{bmatrix} \frac{C_F}{m} & \frac{C_R}{m} \\ \frac{l_F C_F}{I_z} & \frac{-l_R C_R}{I_z} \end{bmatrix}^{-1} \\ & \cdot \begin{bmatrix} -\frac{(C_F + C_R)}{m V_{xref,k+1}} & -V_{xref,k+1} - \frac{(l_F C_F - l_R C_R)}{m V_{xref,k+1}} \\ -\frac{(l_F C_F - l_R C_R)}{I_z V_{xref,k+1}} & -\frac{({l_F}^2 C_F + {l_R}^2 C_R)}{I_z V_{xref,k+1}} \end{bmatrix} \cdot \begin{bmatrix} V_{yref,k+1} \\ r_{ref,k+1} \end{bmatrix} \end{aligned} \tag{2}$$

With the above formulation, it is possible to manipulate the attitude of the vehicle during path-tracking by providing specific references to the controller. Taking the double lane-change manoeuvre for instance, if a constant yaw angle and the corresponding velocity references are given, it is expected to override the nominal steering behaviour, and to carry out the double lane-change manoeuvre with crab steering. This can potentially reduce the yaw motion of the vehicle, and the advantage of crab steering in such scenario is to be investigated.

4 Motion Comfort Evaluation Metrics

In this paper, two metrics are used to evaluate motion comfort with the proposed control strategies, including ride comfort (RC) and motion sickness (MS). Both metrics apply frequency weightings to three-dimensional translational as well as three-dimensional rotational motions, while RC focuses on the higher frequencies which are above 1Hz, and MS focuses on the lower frequencies below 1Hz. According to ISO-2631-1:1997, RC and MS of individual motions can be assessed by combining the Root Mean Square (RMS) values of the weighted accelerations, which can be calculated as:

$$M_i = \left(\frac{1}{t} \int_0^t a_{w_i}^2 d\tau \right)^{\frac{1}{2}}, \tag{3}$$

where M_i stands for RC or MS metric of the specific motion, and a_{w_i} refers to the weighted accelerations in the time domain, which are obtained by:

$$A_{w_i} = WP_i \cdot WA_i \cdot A_i, \tag{4}$$

where A_i refers to the accelerations in the frequency domain, and A_{w_i} are the corresponding weighted accelerations. WP_i and WA_i stand for the principal and additional frequency weightings. For RC, the principal filter for vertical motion and the additional filter for all rotational motions are used as per ISO-2631, while no filters are used for the longitudinal or lateral motion. For MS, since ISO-2631 is lacking in such information, similar process is followed for the calculation of MS metrics, while filters from the literature are used [12–14]. The filters used in this work can be found in [15]. The overall RC and MS metrics can then be calculated by summing the product of M_i and appropriate factors k_i:

$$M = \left(\sum_{i=1}^{6} k_i^2 \cdot M_i^2 \right)^{\frac{1}{2}}. \tag{5}$$

In order to better assess the RC and MS experienced by the passengers on the vehicle, the accelerations are supposed to be in the head reference frame. Hence in this work, the vehicle accelerations obtained from simulation is transformed from the vehicle's body frame to the passengers' head frame with a multi-dimensional human body model. The model includes the seat-to-head transmissibilities from experimental tests and simulation models, and takes into account body induced oscillations, as well as head rotational responses to seat translational and rotational accelerations. Eqs. 6 and 7 demonstrate how such transformation is carried out:

$$a_{xh} = T_{\theta x} \ddot{\theta}, \quad a_{yh} = T_{\phi y} \ddot{\phi}, \quad a_{zh} = T_{\theta z} T_z a_z \tag{6}$$

$$\ddot{\phi}_h = T_\phi \ddot{\phi}, \quad \ddot{\theta}_h = T_\theta \ddot{\theta}, \quad \ddot{\psi}_h = T_{\phi r} T_\psi \ddot{\psi} \tag{7}$$

where a_i and a_{ih} $(i = x, y, z)$ refer to the translational acceleration in vehicle frame and head frame respectively, while $\ddot{j}$ and $\ddot{j}_h$ $(j = \phi, \theta, \psi)$ denote the roll, pitch and yaw accelerations in vehicle frame and head frame. More information of the multi-dimensional human body model can be found in [16].

5 Simulation Results

This section demonstrates the simulation results for evaluating the performance of the developed path-tracking controller. The simulation is carried out with a high-fidelity vehicle model and scenario built in IPG CarMaker, and is run on a laptop powered by Intel Core i7-1185G7 CPU at 3.0 GHz with 32 GB RAM. The vehicle parameters as well as control limitation are given in Table 1. The NMPC optimization problem is solved by FORCESPRO [17]. A sampling time of 0.02 s and prediction horizon of 1 s are used for the NMPC algorithm.

Table 1. System Configuration of the Controllers

Parameter	Value	Parameter	Value
m [kg]	874.5	B	9.50
I_z [kgm^2]	1597.7	C	1.63
l [m]	1.995	D	1.16
l_f [m]	0.815	C_F	91393.39
l_r [m]	1.180	C_R	63123.40
w [m]	1.530	$\delta_{F,lim}$ [deg]	19
w_l [m]	0.765	$\delta_{R,lim}$ [deg]	19
w_r [m]	0.765	$T_{F,lim}$ [Nm]	800
h [m]	0.297	$T_{R,lim}$ [Nm]	350

First the path-tracking performance is evaluated on a double lane-change track defined in ISO 3888-1:2018. A moving average filter is applied on the Y position of the track centre line along the X axis to generate a smooth reference path. Given a reference velocity of 47 m/s, the path-tracking performance with both nominal steering and crab steering is shown in Fig. 2. According to Fig. 2a, at the given reference velocity, the vehicle gets very close to the limits of handling. Figure 2b shows the path-tracking trajectories of the vehicle with nominal and crab steering strategies. Stability is maintained with both strategies, while crab steering is able to achieve a maximum lateral tracking error of 0.297 m, which is smaller than 0.317 m with nominal steering at such extreme condition. On the other hand, the RMS lateral tracking error with nominal steering is 0.103 m, and is smaller than the 0.116 m error with crab steering.

One of the most significant differences between nominal steering and crab steering is in the yaw motion of the vehicle, which is shown in Fig. 2c. Due

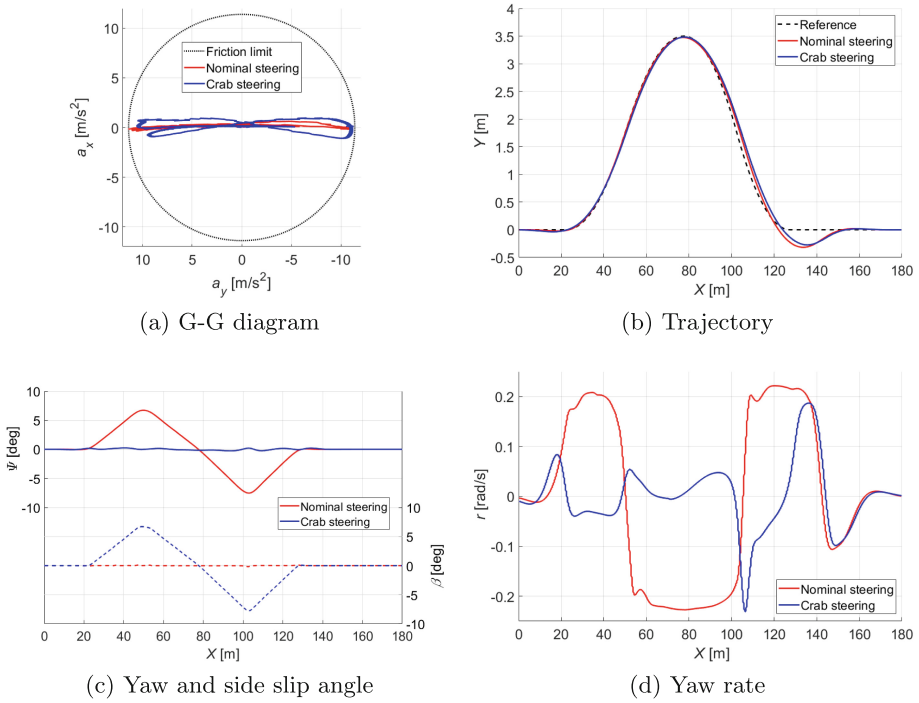

(a) G-G diagram (b) Trajectory

(c) Yaw and side slip angle (d) Yaw rate

Fig. 2. Path-tracking performance with nominal and crab steering strategies in double lane-change manoeuvre at 47 m/s.

to the presence of constant yaw angle reference, the vehicle's yaw angle is kept within 0.3 deg with crab steering. This is smaller than the nominal steering case, while at the same time, larger variation in the side slip angle β can be observed with crab steering. According to Fig. 2d, the yaw rate with crab steering is much smaller as well. The RMS value of yaw rate with crab steering is 0.068 rad/s, which is 58.5% smaller than the 0.164 rad/s with nominal steering.

To investigate how crab steering can affect motion comfort, more simulation are carried out in the double lane-change scenario at different reference velocities, so as to compare the RC and MS metrics with nominal and crab steering strategies. Figure 3 shows the RC metrics with both strategies. The differences between nominal and crab steering in the individual RC metrics due to different acceleration types are demonstrated in Fig. 3a, where a negative ΔRC value means that crab steering has a smaller RC metric than nominal steering. According to the results, the nominal steering has smaller RC metrics in longitudinal and pitch motion, while the application of crab steering improves RC in lateral, roll and yaw motion, due to reduction in the yaw rate and the corresponding load transfer. The overall RC metrics of the two strategies are shown in Fig. 3b. In general, crab steering is able to achieve better RC than nominal steering, and

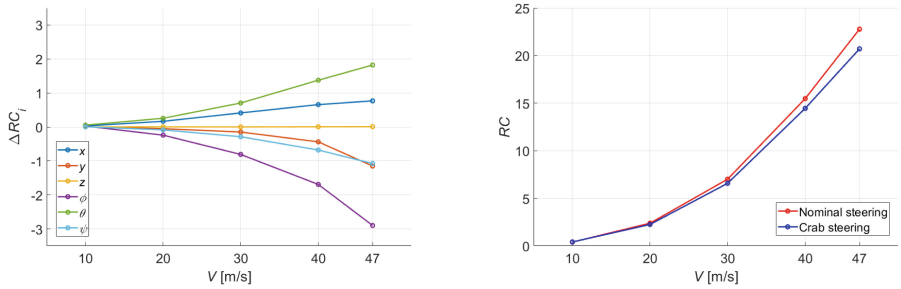

(a) Individual RC difference (b) Overall RC

Fig. 3. RC metrics with nominal and crab steering strategies in double lane-change manoeuvre at different velocities.

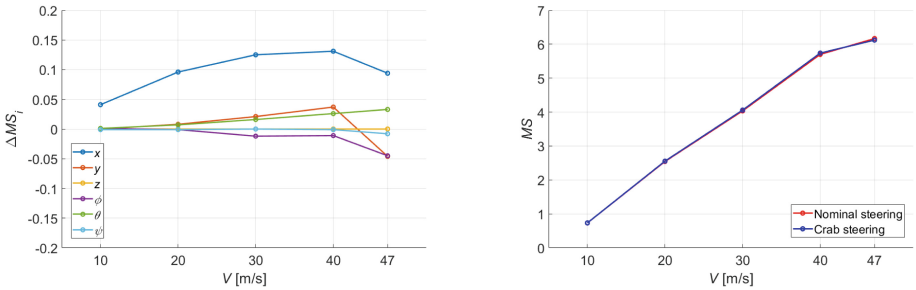

(a) Individual MS difference (b) Overall MS

Fig. 4. MS metrics with nominal and crab steering strategies in double lane-change manoeuvre at different velocities.

the advantage is greater at higher velocity. At 47 m/s, the RC metric of crab steering is 9.1% smaller than nominal steering.

The MS metrics with both strategies are shown in Fig. 4. As shown in Fig. 4a, the MS metric in longitudinal motion with crab steering is slightly higher than nominal steering, while the other individual MS metrics are roughly equivalent between the two strategies. Figure 4b shows the overall MS metrics. The maximum difference between nominal and crab steering takes place at 47 m/s, where the MS metric with crab steering is 0.8% lower. While in general, the difference in MS between the two strategies is negligible.

As double lane-change manoeuvre may not be sufficient to distinguish the differences in RC and MS between nominal and crab steering, a slalom manoeuvre which includes seven of the above double lane-change path is used in the simulation to further explore the effect of crab steering in motion comfort. Reference velocity is given at 30m/s, which is equivalent to the national speed limit on UK motorways. Figure 5 shows the overall RC and MS metrics with nominal and crab steering. RC is reduced by 7.4% with crab steering, which is larger than the results in the double lane-change scenario, where the difference is 6.2%.

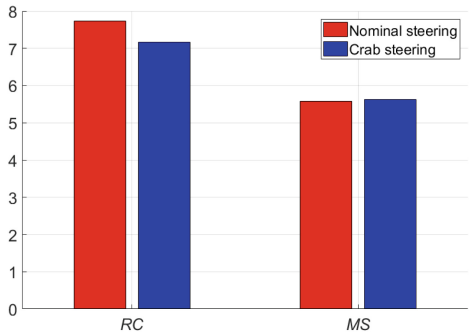

Fig. 5. RC and MS metrics in slalom manoeuvre at 30 m/s with nominal and crab steering.

In terms of MS, the difference in the overall MS metric is 0.7% and hence still negligible. These results further prove that the crab steering strategy is able to improve RC in lane-change manoeuvres, without a noticeable compromise on MS.

Conclusions

In this paper, an NMPC controller is presented for the path-tracking purpose of AVs. The control development is based on a nonlinear double-track vehicle model, and is formulated in a way to allow the manipulation of vehicle attitude during path-tracking. With the application of AWS, crab steering behaviour can be carried out with an additional yaw angle reference. The developed controller is validated in simulation, and the crab steering strategy is compared with nominal steering in the aspects of path-tracking performance and motion comfort. According to the simulation results in a double lane-change scenario, vehicle with crab steering has a slightly larger RMS lateral tracking error by 0.013 m at the limit handling condition, while the maximum tracking error with crab steering is 0.02 m smaller than the nominal-steering behaviour. Furthermore, crab steering can significantly reduce the yaw rate by 58.5%. Although such great impact on the yaw rate is not fully depicted in the enhancement of motion comfort due to the applied filters (WP_i and WA_i, Eq. 4) and weighting coefficients (k_i, Eq. 5), it can still be observed by comparing both strategies at different velocities that the application of crab steering is able to improve ride comfort and maintain the same level of motion sickness compared with nominal steering. The improvement in ride comfort is greater at higher velocity, up to 9.1% at the limit handling condition, while the difference in MS metric remains smaller than 1%. In addition, the advantage of crab steering in enhanced ride comfort is also confirmed in a slalom scenario.

Acknowledgments. This work is supported by Innovate UK under the AID-CAV project (project reference 104277). The authors confirm that the data supporting this study are included within the article.

References

1. Yao, Q., Tian, Y., Wang, Q., Wang, S.: Control strategies on path tracking for autonomous vehicle: state of the art and future challenges. IEEE Access **8**, 161211–161222 (2020)
2. Rokonuzzaman, M., Mohajer, N., Nahavandi, S., Mohamed, S.: Review and performance evaluation of path tracking controllers of autonomous vehicles. IET Intell. Transp. Syst. **15**(5), 646–670 (2021)
3. Yu, R., Guo, H., Sun, Z., Chen, H.: Mpc-based regional path tracking controller design for autonomous ground vehicles. In: 2015 IEEE International Conference on Systems, Man, and Cybernetics, pp. 2510–2515 (2015)
4. Siampis, E., Velenis, E., Longo, S.: Model predictive torque vectoring control for electric vehicles near the limits of handling. In: 2015 European Control Conference (ECC), pp. 2553–2558 (2015)
5. Chen, T., Chen, L., Xu, X., Cai, Y., Sun, X.: Simultaneous path following and lateral stability control of 4wd-4ws autonomous electric vehicles with actuator saturation. Adv. in Eng. Softw. **128**, 46–54 (2019)
6. Wang, R., Yin, G., Zhuang, J., Zhang, N., Chen, J.: The path tracking of four-wheel steering autonomous vehicles via sliding mode control. In: 2016 IEEE Vehicle Power and Propulsion Conference (VPPC), pp. 1–6 (2016)
7. Acosta, M., Kanarachos, S., Fitzpatrick, M.E.: On full magv lateral dynamics exploitation: Autonomous drift control. In: 2018 IEEE 15th International Workshop on Advanced Motion Control (AMC), pp. 529–534 (2018)
8. Htike, Z., Papaioannou, G., Siampis, E., Velenis, E., Longo, S.: Minimisation of motion sickness in autonomous vehicles. In: 2020 IEEE Intelligent Vehicles Symposium (IV), pp. 1135–1140 (2020)
9. Liu, Q., Song, S., Hu, H., Huang, T., Li, C., Zhu, Q.: Extended model predictive control scheme for smooth path following of autonomous vehicles. Front. of Mech. Eng. **17**(4) (2022)
10. Jeong, Y., Yim, S.: Path tracking control with four-wheel independent steering, driving and braking systems for autonomous electric vehicles. IEEE Access **10**, 74733–74746 (2022)
11. Lin, C., Siampis, E., Velenis, E.: Real-time path-tracking mpc for an over-actuated autonomous electric vehicle. In: 2022 American Control Conference (ACC), pp. 2006–2011 (2022)
12. Griffin, M.J., Mills, K.L.: Effect of frequency and direction of horizontal oscillation on motion sickness. Aviat. Space Environ. Med. **73**(6), 537–543 (2002)
13. Donohew, B.E., Griffin, M.J.: Motion sickness: effect of the frequency of lateral oscillation. Aviat. Space Environ. Med. **75**(8), 649–656 (2004)
14. Howarth, H.V.C., Griffin, M.J.: Effect of roll oscillation frequency on motion sickness. Aviat. Space Environ. Med. **74**(4), 326–331 (2003)
15. Papaioannou, G., Zhao, L., Nybacka, M., Jerrelind, J., Happee, R., Drugge, L.: Motion comfort and driver feel: an explorative study about their relation in remote driving. Arxiv (2023)

16. Papaioannou, G., Jerrelind, J., Drugge, L., Shyrokau, B.: Assessment of optimal passive suspensions regarding motion sickness mitigation in different road profiles and sitting conditions. In: 2021 IEEE International Intelligent Transportation Systems Conference (ITSC), pp. 3896–3902 (2021)
17. Zanelli, A., Domahidi, A., Jerez, J., Morari, M.: Forces NLP: an efficient implementation of interior-point methods for multistage nonlinear nonconvex programs. Int. J. of Control **93**(1), 13–29 (2020)